Distinct response of adult neural stem cells to low versus high dose ionising radiation.

Barazzuol, Lara; Hopkins, Suzanna R.; Ju, Limei; Jeggo, Penelope A.

Published in:
Dna repair

DOI:
10.1016/j.dnarep.2019.01.004

Publication date:
2019

DNA Repair 76 (2019) 70–75

Contents lists available at ScienceDirect

DNA Repair

journal homepage: www.elsevier.com/locate/dnarepair

Distinct response of adult neural stem cells to low versus high dose ionising radiation

Lara Barazzuol[a,b,*], Suzanna R. Hopkins[c], Limei Ju[c], Penelope A. Jeggo[c]

[a] Department of Radiation Oncology, University of Groningen, University Medical Center Groningen, Groningen 9700 RB, the Netherlands
[b] Department of Biomedical Sciences of Cells and Systems, Section of Molecular Cell Biology, University of Groningen, University Medical Center Groningen, Groningen 9713 AV, the Netherlands
[c] Genome Damage and Stability Centre, School of Life Sciences, University of Sussex, Brighton BN1 9RQ, UK

ARTICLE INFO

Keywords:
Neural stem cells
Low dose radiation
DNA damage response

ABSTRACT

Radiosusceptibility is the sensitivity of a biological organism to ionising radiation (IR)-induced carcinogenesis, an outcome of IR exposure relevant following low doses. The tissue response is strongly influenced by the DNA damage response (DDR) activated in stem and progenitor cells. We previously reported that *in vivo* exposure to 2 Gy X-rays activates apoptosis, proliferation arrest and premature differentiation in neural progenitor cells (transit amplifying cells and neuroblasts) but not in neural stem cells (NSCs) of the largest neurogenic region of the adult brain, the subventricular zone (SVZ). These responses promote adult quiescent NSC (qNSC) activation after 2 Gy. In contrast, neonatal (P5) SVZ neural progenitors continue proliferating and do not activate qNSCs. Significantly, the human and mouse neonatal brain is radiosusceptible.

Here, we examine the response of stem and progenitor cells in the SVZ to low IR doses (50–500 mGy). We observe a linear dose-response for apoptosis but, in contrast, proliferation arrest and neuroblast differentiation require a threshold dose of 200 or 500 mGy, respectively. Importantly, qNSCs were not activated at doses below 500 mGy. Thus, full DDR activation in the neural stem cell compartment *in vivo* necessitates a threshold dose, which can be considered of significance when evaluating IR-induced cancer risk and dose extrapolation.

1. Introduction

A DNA double strand break (DSB) is the biologically relevant DNA damage induced by ionising radiation (IR). At high IR doses, radiosensitivity arises from the lethal impact of DSBs. Indeed, human patients, mice and cells deficient in DSB repair show marked radiosensitivity [1,2]. However, aside from radiotherapy for cancer treatment, we are not usually exposed to high IR doses. In contrast, the human population is receiving increasing exposure to low dose IR due to medical X-ray imaging, computed tomography (CT)-scanning for diagnostic purposes and long-haul flights [3–5]. One outcome of low dose exposure is carcinogenesis rather than cell killing, which can potentially arise via DSB mis-repair, such as balanced chromosomal translocation formation. Sensitivity to IR-induced carcinogenesis has recently been defined as radiosusceptibility (compared to radiosensitivity, which represents sensitivity to the killing effects of IR) [6]. We will use this nomenclature here. Assessing risks to carcinogenesis from low doses is extremely difficult given the lack of a well-defined signature for IR-induced cancers, and that X-ray-treated individuals may have underlying cancer pre-disposing health effects. Currently, risk estimations for radiation exposure have relied on a linear non-threshold dose-response, albeit subject to considerable debate [7,8]. An important consideration is whether the response to DNA damage (DDR), particularly those responses protective against carcinogenesis, arise linearly with dose. For example, previous studies using cultured cells have shown that G2/M checkpoint arrest requires a threshold dose for activation [9,10].

For considering radiosusceptibility, the DDR activated in stem and progenitor cells is particularly important although our understanding of the DDR in stem compared to differentiated cells is poor, while evidence suggests that there are distinctions [11–15]. We previously analysed the DDR activated by 2 Gy IR in neural stem cells (NSCs) in the subventricular zone (SVZ), the largest germinal zone in the adult forebrain, which can promote neurogenesis during adulthood [16]. Type B adult NSCs express Glial Fibrillary Acidic Protein (GFAP). They are predominantly quiescent with only 5–10% expressing Ki67, a proliferation marker. They produce further NSCs via symmetric division and undergo asymmetric division generating type C transit amplifying

* Corresponding author.
E-mail address: l.barazzuol@umcg.nl (L. Barazzuol).

https://doi.org/10.1016/j.dnarep.2019.01.004
Received 30 October 2018; Received in revised form 15 January 2019; Accepted 17 January 2019
Available online 18 January 2019

progenitors (TAPs). TAPs undergo further symmetric division prior to asymmetric division generating neuroblasts (NBs; also called type A cells) which express the doublecortin (Dcx) marker. NBs subsequently migrate through the rostral migratory stream to the olfactory bulb, where they differentiate into mature interneurons. We previously exploited insight into the SVZ substructure, delineating four subdomains designated as dorsal, medial, ventral and dorsolateral [17]. The subdomains differ in their age-dependent proliferative capacity. Significantly, in adult mice (3-month-old), progenitor cells were almost absent in the medial and dorsal subdomains, providing a useful resource to assess the IR response of quiescent NSCs (qNSCs) versus progenitor cells. Importantly, we found that IR-induced apoptosis was only activated in zones encompassing progenitor cells, demonstrating that neither qNSCs nor activated NSCs (aNSCs) undergo IR-induced apoptosis. We also identified two novel responses in neural progenitor (NP) cells (TAPs and NBs), namely proliferation arrest and loss of the neuroblast marker via premature differentiation [16]. Importantly, the activation of these responses was ATM-dependent and caused qNSC activation, which was similarly ATM-dependent. Importantly, after 2 Gy, proliferation arrest in NPs appeared to be permanent with progenitor replenishment arising by qNSC activation. We concluded that after 2 Gy IR, NPs were removed by three responses (apoptosis, proliferation arrest and premature differentiation) with new progenitors arising 1–2 weeks post-exposure via qNSC activation. Proliferation with damaged DNA can compound or fix the damage. Hence removal of progenitors could facilitate the elimination of radiosusceptible cells. qNSCs commenced proliferation after some delay, when repair was likely completed. Significantly, in the neonatal SVZ, which is sensitive to carcinogenesis in mice and humans [18–21], we observed transient and diminished proliferation arrest and no significant qNSC activation. Importantly, a recent study has identified driver mutations for glioblastoma in the adult human NSCs, which then migrate from the SVZ to develop into high-grade malignant gliomas, thereby identifying mutations arising in the NSCs in the SVZ as the origin of brain tumours [22].

Here, we examine these responses following low dose IR exposure. Consistent with previous findings [23,24], we found that apoptosis arises linearly with dose from 50 to 500 mGy in progenitor cells. In contrast, activation of proliferation arrest and Dcx marker loss required defined thresholds of 200 or 500 mGy, respectively. Moreover, even after 200 or 500 mGy, the duration of arrest was transient. qNSC activation necessitated doses greater than 200 mGy. Collectively, these findings demonstrate that two important DDRs, proliferation arrest and stem cell differentiation, require a threshold activation dose and are inefficiently activated at low doses. These responses provide a route to remove damaged progenitors. Thus, not all DDRs in stem cells, an important cell type for considering carcinogenesis, can be extrapolated from high to low radiation doses.

2. Materials and methods

2.1. Mice

Three-month old wild type (129/SV x C57BL/6) mice were designated as adult mice. Animal experiments were performed in accordance with accepted standards of animal welfare approved by the United Kingdom Home Office and complied with the Animals (Scientific Procedures) Act 1986.

2.2. Irradiation

Animals received whole body irradiation using an HS X-ray system (A.G.O. installation, UK) at a dose rate of 0.5 Gy/min and a 250 kV potential with doses from 0.05 to 2 Gy.

2.3. Topographical analysis

The SVZ subdomain division was undertaken as described previously [16,17]. Briefly, the SVZ was divided along the ventral-dorsal axis into ventral, medial, dorsal and dorsolateral subdomains. Analysis focused on the ventral and dorsolateral subdomains, which are proliferating in adult (3-month-old) mice [16].

2.4. Immunostaining

Brains were fixed in 4% paraformaldehyde (Santa Cruz Biotecnology, cat#SC-281692) for 48 h at +4C and subsequently cryoprotected in 25% sucrose, frozen after OCT embedding (Thermo Fisher Scientific, cat#12678646) and stored at -80C. Brains were sectioned using a Leica Cryostat at a thickness of 7 μm and mounted on SuperFrost Plus slides (Thermo Fisher Scientific, cat#10149870) or TOMO adhesive slides (Matsunami, cat#TOM-11). Slides were re-equilibrated at room temperature (RT) for 30 min, then washed in PBS for 10 min and placed in a coplin jar containing the antigen retrieval solution (Histo-VT-One, Fine Chemicals Products Ltd, cat#06380-05), heated using a microwave, and incubated in the heated solution for 1 h. Tissue sections were washed three times in PBS and blocked in 5% serum (donkey or goat), 1% bovine serum albumin (BSA) and 0.4% Triton X-100 in PBS for 1 h at RT. After blocking, tissue sections were incubated with the primary antibody diluted in blocking solution overnight in humified chamber at either RT or +4C. The following primary antibodies were used: Dcx (goat, 1:400, Santa Cruz Biotechnology, cat#sc-8066), GFAP (rabbit, 1:500, Dako, cat#Z0334) and Ki67 (rat, 1:500, Thermo Fisher Scientific, eBioscience, cat#14-5698-80). Tissue sections were subsequently washed 3 times in PBS and incubated with the relative Alexa Fluor-conjugated secondary antibodies (Thermo Fisher Scientific) diluted in blocking buffer at 1:500 for 1 h at RT. Tissue sections were counterstained with DAPI and mounted with 80% glycerol or Dako mounting medium (Agilent Dako, cat#S3025).

2.5. Assessment of apoptosis using TUNEL

TUNEL staining was performed according to the manufacturer's instructions (Roche, cat#11684795910-2156792910).

3. Results

3.1. Apoptosis arises linearly with dose from 50 to 500 mGy in the adult SVZ

For most analysis, we sub-divided the SVZ into the ventral, dorsolateral, medial and dorsal subdomains, as described previously (Fig. 1A). Significantly, proliferating cells and IR-induced apoptotic cells were predominantly observed only in the ventral and dorsolateral subdomains. However, for our assessment of apoptosis, we assessed the total number of cells per lateral ventricle (LV) without distinguishing the response of individual subdomains. To assess apoptosis in the adult SVZ, we exposed adult mice to 50–500 mGy X-rays, and monitored $TUNEL^+$ cells per LV at 6 h after irradiation. 6 h was chosen as the time showing maximal $TUNEL^+$ cells [23,24]. The number of $TUNEL^+$ cells increased linearly with dose, fitting a linear-no-threshold model (Fig. 1B-D). These results are consistent with our study of the embryonic neocortex, where we similarly observed a linear dose-response [24,25].

3.2. A dose of 200 mGy is required for efficient proliferation arrest

We previously reported that after 2 Gy, NPs (TAPs and NBs) in the adult SVZ cease proliferation and lose their Ki67 proliferation marker by 6 h post irradiation. This proliferation arrest was prolonged, lasting

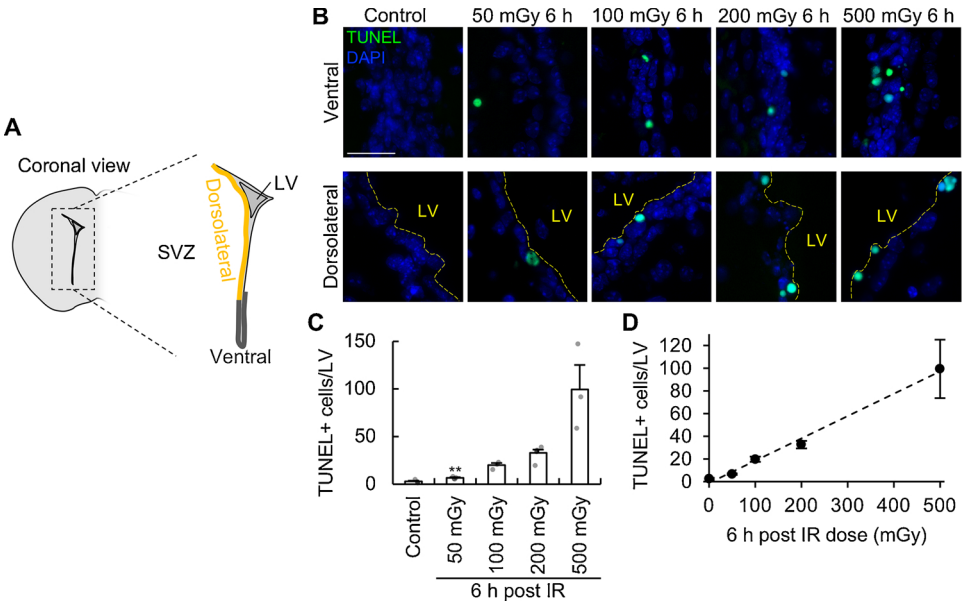

Fig. 1. Apoptosis is linearly induced at low radiation doses. (**A**) Schematic coronal representation of the SVZ showing the ventral (grey) and dorsolateral (yellow) subdomains. This colour code will be used in this and all subsequent figures. (**B**) Representative images of the ventral and dorsolateral subdomains of untreated control mice or at 6 h after exposure to radiation doses from 50 to 500 mGy stained with TUNEL (green) and DAPI (blue). (**C**) Quantification of the number of TUNEL$^+$ cells per lateral ventricle (LV) in control and irradiated mice at 6 h post 50 to 500 mGy. (**D**) Linear fitting of the data presented in panel C. Experiments were carried out on 3 month-old mice and represent the mean ± SEM of n ≥ 3 mice for each condition. Scale bars, 25 µm. Student's t-test, **P ≤ 0.01.

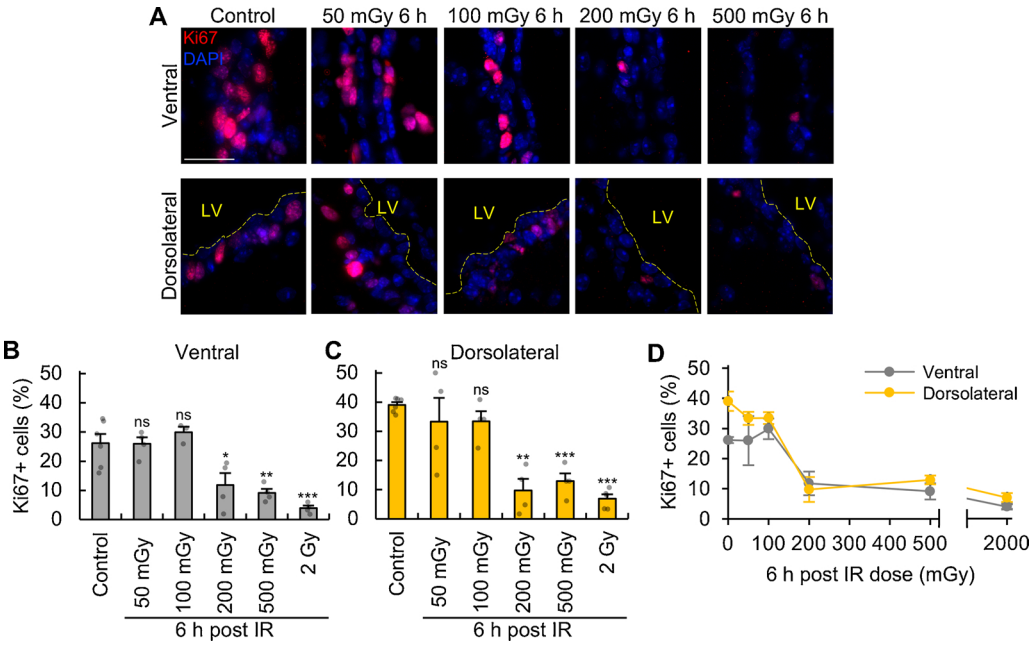

Fig. 2. Proliferation arrest has a threshold dose of 200 mGy. Representative images (**A**) and quantification (**B**, **C**) of the ventral and dorsolateral subdomains of untreated control mice or at 6 h after exposure to radiation doses from 50 to 500 mGy stained with Ki67 (red) and DAPI (blue). The percentages are normalized to the number of DAPI positive cells. (**D**) Dose-response relationship of the data presented in panels B and C between the radiation dose (presented in mGy) and the percentage of proliferating Ki67$^+$ cells in the ventral and dorsolateral subdomains at 6 h after irradiation. Note that a break was applied to the x-axis to display the response to 2000 mGy. Experiments represent the mean ± SEM of n ≥ 3 mice for each condition. Scale bars, 25 µm. Student's t-test, *P ≤ 0.05, **P ≤ 0.01, ***P ≤ 0.001, n.s. not significant. Data at 2 Gy were as previously published [16].

over 48 h [16]. Here, we analysed the response to low IR doses focusing on the ventral and dorsolateral SVZ subdomains, which show the highest density of aNSCs and NPs. We found that doses of 100 mGy or less failed to initiate proliferation arrest (assessed using the Ki67 marker) in either subdomain (Fig. 2A-C). In contrast, proliferation arrest occurred efficiently following exposure to 200 or 500 mGy. The data presented as a dose-response highlight the presence of a defined dose threshold of 200 mGy above which proliferation arrest occurs efficiently with no significant arrest being observed at lower doses (Fig. 2D).

3.3. The duration of proliferation arrest is dose dependent

Next, we examined the duration of proliferation arrest. Our previous work showed that exposure to 2 Gy confers prolonged proliferation arrest [16], which is maintained for 48 h. In contrast, following exposure to 200 and 500 mGy, cells within the ventral or dorsolateral subdomains were maximally arrested at 6 h post irradiation but recovery was detectable by 24 or 48 h (Fig. 3A-C). The level of proliferating Ki67$^+$ cells increased more rapidly in the dorsolateral than in the ventral subdomain (Fig. 3B-C). As shown above, no proliferation arrest was observed at 6 h (or at 24 h) after 50 or 100 mGy. Thus, the duration of proliferation arrest is dose dependent, with higher doses causing prolonged arrest.

3.4. Low dose IR does not promote premature differentiation

We previously found that proliferation arrest was coupled with premature neuronal differentiation of NBs (expressing the immature neuronal marker Dcx) after 48 h in the adult SVZ exposed to 2 Gy [16]. To assess the effect of low dose IR on differentiation, we measured the Dcx$^+$ NBs via immunofluorescence at 24 and 48 h following 200 and 500 mGy X-rays (Fig. 3D-E). The data presented as a dose-response at 48 h (Fig. 3F) show that after 200 mGy the percentage of Dcx$^+$ cells did not significantly change compared to control levels in the ventral or dorsolateral subdomains, whereas at 24 and 48 h after 500 mGy X-rays,

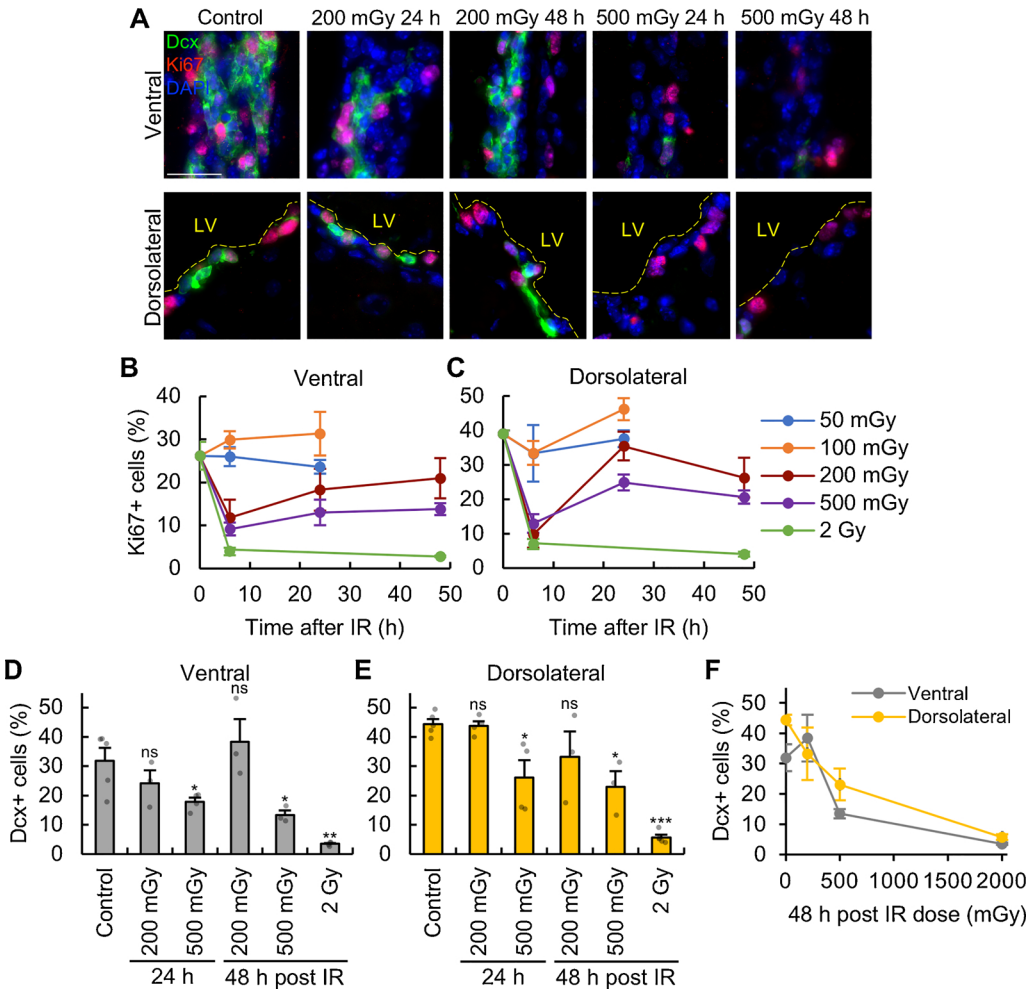

Fig. 3. Loss of Dcx marker expression occurs at doses greater than 500 mGy. (**A**) Representative images of the ventral and dorsolateral subdomains of untreated control mice or at 24 and 48 h after exposure to radiation doses of 200 or 500 mGy stained with Dcx (green), Ki67 (red) and DAPI (blue). Kinetics of Ki67 expression in the ventral (**B**) and dorsolateral (**C**) subdomains of the SVZ at different time points after irradiation in mice exposed to doses from 50 mGy to 2 Gy. Quantification of Dcx^+ cells in the ventral (**D**) and dorsolateral (**E**) SVZ subdomains at 24 and 48 h after irradiation with 200 mGy, 500 mGy and 2 Gy. (**F**) Dose-response relationship of the data presented in panels D and E between the radiation dose (presented in mGy) and the percentage of Dcx^+ cells in the ventral and dorsolateral subdomains at 48 h after irradiation. Experiments represent the mean ± SEM of n ≥ 3 mice for each condition. Scale bars, 25 μm. Student's t-test, $^*P \leq 0.05$, $^{**}P \leq 0.01$, $^{***}P \leq 0.001$, n.s. not significant. Data at 2 Gy were as previously published [16].

the percentage of Dcx^+ cells significantly decreased in both subdomains. Although there appears to be a small loss of Dcx^+ cells at 48 h after 200 mGy in the dorsolateral subdomain, this difference was not significant and was not evident at 24 h (Fig. 3D-E). Interestingly, the loss of Dcx^+ cells was more pronounced in the ventral subdomain, where loss of proliferation was maintained for a longer period compared with the dorsolateral subdomain. These findings show that low IR doses, which induce only transient proliferation arrest, do not promote premature differentiation.

3.5. Proliferation arrest and differentiation are required to promote quiescent NSC activation

The adult SVZ region largely consists of qNSCs, which can become activated to maintain tissue homeostasis or promote repair during injury. aNSCs can be identified as $Ki67^+GFAP^+$ cells and in untreated 3-month-old mice approximately 10% of the $GFAP^+$ cells are $Ki67^+$ [16]. Previous studies demonstrated that qNSCs start cycling 4 days after exposure to doses greater than 2 Gy [26]. Here, we similarly observed that at 4 and 7 days after 500 mGy, qNSCs become activated as shown by the increased percentage of $GFAP^+Ki67^+$ among the $GFAP^+$ cells (Fig. 4). Consistent with the proliferation arrest data (Fig. 3B-C), the transition from quiescence to activation was more prominent in the dorsolateral subdomain (Fig. 4C). In contrast, there was no significant activation of qNSCs after doses less than 500 mGy at either 4 or 7 days post irradiation (Fig. 4B-D).

4. Discussion

A dose of 100–200 mGy is required to activate and maintain IR-induced G2/M checkpoint arrest in human fibroblasts [10,27]. Such work has established the concept that a threshold dose is required to activate specific DDRs, which impact upon the maintenance of genomic stability. Here, we examine the DDR in neuronal stem and progenitor cells after low IR doses to determine whether they arise linearly with dose or have a defined activation threshold. Consistent with findings in the embryonic SVZ, apoptosis in the adult SVZ has a linear dose-response from 50 to 500 mGy. Assuming that 1 Gy induces ~ 25–40 DSBs, this suggests that 1–2 DSBs/cell is sufficient to activate apoptosis albeit at a low frequency. In stark contrast, proliferation arrest has a defined threshold, being observed at a similar magnitude after 200 mGy or 2 Gy but not after 100 mGy. Moreover, the duration of arrest is more transient after 200 and 500 mGy compared to that observed after 2 Gy. This distinction is striking, particularly in the dorsolateral subdomain. We previously provided strong evidence that NBs prematurely differentiate after 2 Gy since only 50% of Dcx^+ cells undergo apoptosis whilst Dcx^+ cell numbers diminish more than tenfold [16]. Premature differentiation was confirmed by an increase in $Tuj1^+$ and $Map2^+$ cells, the major differentiated derivative of Dcx^+ cells. The apoptotic level is low after 500 mGy and cannot provide the sole explanation for the diminished Dcx^+ cell numbers. Premature differentiation, potentially coupled with proliferation arrest, provides a likely explanation. Strikingly, after 200 mGy, proliferation arrest is similar to that observed after 500 mGy yet Dcx^+ cells do not significantly decrease, strongly suggesting that premature differentiation does not arise. It is possible that prolonged

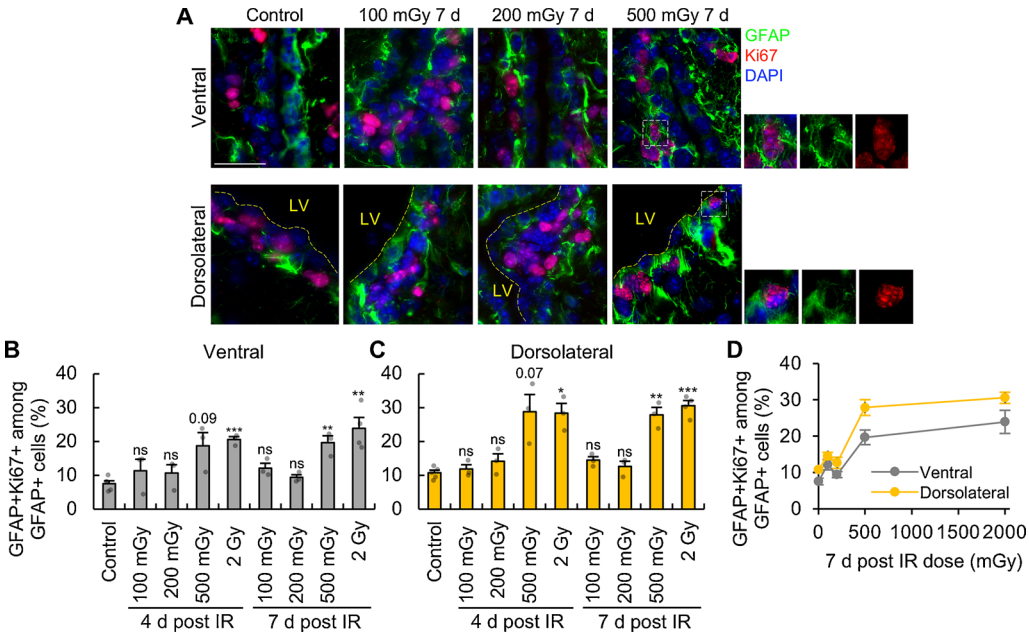

Fig. 4. A dose of 500 mGy is required for the transition of NSCs from quiescence to activation. (**A**) Representative images of the ventral and dorsolateral subdomains of untreated control mice and at 7 days after exposure to radiation doses of 100, 200 and 500 mGy stained with GFAP (green), Ki67 (red) and DAPI (blue). Quantification of aNSCs as measured by the percentage of $GFAP^+Ki67^+$ cells among the $GFAP^+$ cells in the ventral (**B**) and dorsolateral (**C**) subdomains of control and irradiated mice with 100, 200, 500 mGy and 2 Gy at 4 and 7 days post irradiation. (**D**) Dose-response relationship of the data presented in panels B and C between the radiation dose (presented in mGy) and the percentage of aNSCs in the ventral and dorsolateral subdomains at 7 days after radiation exposure. Experiments represent the mean ± SEM of n ≥ 3 mice for each condition. Scale bars, 25 μm. Student's t-test, *P ≤ 0.05, **P ≤ 0.01, ***P ≤ 0.001, n.s. not significant. Data at 7 days after 2 Gy were as previously published [16].

proliferation arrest activates premature differentiation, providing a relationship between these end-points, although, as discussed above, there is some uncoupling between the two responses. It is also possible that cell death of the differentiated neurons causes compensatory differentiation to maintain homeostasis, a feature reported in the Patched heterozygous mouse cerebellum [28]. This, however, seems unlikely since we have not observed any apoptosis in differentiated neurons and other mechanisms of cell death take longer than 48 h, the time when Dcx^+ cell loss can be observed. Finally, an increase in aNSCs is observed after 500 but not 200 mGy. Within a stem cell compartment, loss of progenitors can trigger quiescent stem cell activation promoting progenitor replenishment from cells which were non-proliferating when damaged. Since non-cycling G0 phase cells show enhanced survival and fewer translocations than cycling cells after IR [29], this may diminish the possibility of IR-induced mutational events.

5. Conclusions

In summary, we examine components of the DDR in neural stem and progenitor cells after low dose IR and provide evidence that, whilst apoptosis arises in a dose dependent manner, other critical DDR processes require a defined threshold for activation. These findings are important when evaluating the risk of low dose IR exposure and considering dose-response relationships.

Conflict of interest

No competing interests to declare.

Data availability

All source data are provided in full in the results section of this paper.

Funding

This work was supported by EU 7th Framework Programme (FP7) RISK-IR project (grant number 323267); Medical Research Council (grant numbers G1000050, G0500897). Funding for open access charge: Medical Research Council (G1000050, G0500897, both to PAJ).

References

[1] R. Hakem, DNA-damage repair; the good, the bad, and the ugly, EMBO J. 20 (2008) 589–605.
[2] L. Woodbine, A.R. Gennery, P.A. Jeggo, The clinical impact of deficiency in DNA non-homologous end-joining, DNA Repair (Amst.) 16 (2014) 84–96.
[3] A. Berrington de González, S. Darby, Risk of cancer from diagnostic X-rays: estimates for the UK and 14 other countries, Lancet 363 (2004) 345–351.
[4] M.S. Pearce, J.A. Salotti, M.P. Little, K. McHugh, C. Lee, K. Pyo Kim, N.L. Howe, C.M. Ronckers, P. Rajaraman, A.W. Craft, L. Parker, A. Berrington de González, Radiation exposure from CT scans in childhood and subsequent risk of leukaemia and brain tumours: a retrospective cohort study, Lancet 380 (2012) 499–505.
[5] D. Silverman, M. Gendreau, Medical issues associated with commercial flights, Lancet 373 (2009) 2067–2077.
[6] M. Britel, M. Bourguignon, N. Foray, The use of the term' radiosensitivity' through history of radiation: from clarity to confusion, Int. J. Radiat. Biol. 94 (2018) 503–512.
[7] M. Tubiana, L.E. Feinendegen, C. Yang, J.M. Kaminski, The linear No-Threshold relationship is inconsistent with radiation biologic and experimental data, Radiology 251 (2009) 13–22.
[8] W.M. Bonner, Phenomena leading to cell survival values which deviate from linear-quadratic models, Mutat. Res. 568 (2004) 33–39.
[9] M. Löbrich, P.A. Jeggo, The impact of a negligent G2/M checkpoint on genomic instability and cancer induction, Nat. Rev. Cancer 7 (2007) 861–869.
[10] D. Deckbar, P.A. Jeggo, M. Lobrich, Understanding the limitations of radiation-induced cell cycle checkpoints, Crit. Rev. Biochem. Mol. Biol. 46 (2011) 271–283.
[11] A. Insinga, A. Cicalese, M. Faretta, B. Gallo, L. Albano, S. Ronzoni, L. Furia, A. Viale, P.G. Pelicci, DNA damage in stem cells activates p21, inhibits p53, and induces symmetric self-renewing divisions, Proc. Natl. Acad. Sci. U. S. A. 110 (2013) 3931–3936.
[12] N. Barker, Adult intestinal stem cells: critical drivers of epithelial homeostasis and regeneration, Nat. Rev. Mol. Cell Biol. 15 (2014) 19–33.
[13] P.A. Sotiropoulou, A. Candi, G. Mascré, S. De Clercq, K.K. Youssef, G. Lapouge, E. Dahl, C. Semeraro, G. Denecker, J.C. Marine, C. Blanpain, Bcl-2 and accelerated DNA repair mediates resistance of hair follicle bulge stem cells to DNA-damage-induced cell death, Nat. Cell Biol. 12 (2010) 572–582.
[14] P.W. Nagle, N.A. Hosper, L. Barazzuol, A.L. Jellema, M. Baanstra, M.J. van Goethem, S. Brandenburg, U. Giesen, J.A. Langendijk, P. van Luijk, R.P. Coppes, Lack of DNA damage response at low radiation doses in adult stem cells contributes to organ dysfunction, Clin. Cancer Res. (2018) [Epub ahead of print].
[15] I. Vitale, G. Manic, R. De Maria, G. Kroemer, L. Galluzzi, DNA damage in stem cells, Mol. Cell 66 (2017) 306–319.
[16] L. Barazzuol, L. Ju, P.A. Jeggo, A coordinated DNA damage response promotes adult quiescent neural stem cell activation, PLoS Biol. 15 (2017) e2001264.
[17] R. Fiorelli, K. Azim, B. Fischer, O. Raineteau, Adding a spatial dimension to post-natal ventricular-subventricular zone neurogenesis, Development 142 (2015) 2109–2120.
[18] S. Adeberg, L. König, T. Bostel, S. Harrabi, T. Welzel, J. Debus, S.E. Combs,

Glioblastoma recurrence patterns after radiation therapy with regard to the subventricular zone, Int. J. Radiat. Oncol. Biol. Phys. 90 (2014) 886–893.
[19] L. Chen, K.L. Chaichana, L. Kleinberg, X. Ye, A. Quinones-Hinojosa, K. Redmond, Glioblastoma recurrence patterns near neural stem cell regions, Radiother. Oncol. 116 (2015) 294–300.
[20] A.M. Mistry, A.T. Hale, L.B. Chambless, K.D. Weaver, R.C. Thompson, R.A. Ihrie, Influence of glioblastoma contact with the lateral ventricle on survival: a meta-analysis, J. Neurooncol. 131 (2017) 125–133.
[21] E.Y. Qin, D.D. Cooper, K.L. Abbott, J. Lennon, S. Nagaraja, A. Mackay, C. Jones, H. Vogel, P.K. Jackson, M. Monje, Neural precursor-derived pleiotrophin mediates subventricular zone invasion by glioma, Cell 170 (2017) 845–859.
[22] J.H. Lee, J.E. Lee, J.Y. Kahng, S.H. Kim, J.S. Park, S.J. Yoon, J.Y. Um, W.K. Kim, J.K. Lee, J. Park, E.H. Kim, J.H. Lee, J.H. Lee, W.S. Chung, Y.S. Ju, S.H. Park, J.H. Chang, S.G. Kang, J.H. Lee, Human glioblastoma arises from subventricular zone cells with low-level driver mutations, Nature 560 (2018) 243–247.
[23] L. Barazzuol, N. Rickett, L. Ju, P.A. Jeggo, Low levels of endogenous or X-ray-induced DNA double-strand breaks activate apoptosis in adult neural stem cells, J. Cell. Sci. 128 (2015) 3597–3606.
[24] L. Barazzuol, P.A. Jeggo, In vivo sensitivity of the embryonic and adult neural stem cell compartments to low-dose radiation, J. Radiat. Res. 57 (2016) i2–i10.
[25] S. Saha, L. Woodbine, J. Haines, M. Coster, N. Ricket, L. Barazzuol, E. Ainsbury, Z. Sienkiewicz, P. Jeggo, Increased apoptosis and DNA double-strand breaks in the embryonic mouse brain in response to very low-dose X-rays but not 50 Hz magnetic fields, J. R. Soc. Interface 11 (2014) 20140783.
[26] M. Daynac, A. Chicheportiche, J.R. Pineda, L.R. Gauthier, F.D. Boussin, M.A. Mouthon, Quiescent neural stem cells exit dormancy upon alteration of GABAAR signaling following radiation damage, Stem Cell Res. 11 (2013) 516–528.
[27] D. Deckbar, J. Birraux, A. Krempler, L. Tchouandong, A. Beucher, S. Walker, T. Stiff, P. Jeggo, M. Löbrich, Chromosome breakage after G2 checkpoint release, J. Cell Biol. 176 (2007) 749–755.
[28] M. Mancuso, E. Pasquali, S. Leonardi, M. Tanori, S. Rebessi, V. Di Majo, S. Pazzaglia, M.P. Toni, M. Pimpinella, V. Covelli, A. Saran, Oncogenic bystander radiation effects in Patched heterozygous mouse cerebellum, Proc. Natl. Acad. Sci. U. S. A. 105 (2008) 12445–12450.
[29] M.N. Cornforth, J.S. Bedford, A quantitative comparison of potentially lethal damage repair and the rejoining of interphase chromosome breaks in low passage normal human fibroblasts, Radiat. Res. 111 (1987) 385–405.